Rapid and selective extraction, isolation, preconcentration, and quantitation of small RNAs from cell lysate using on-chip isotachophoresis

Reto B. Schoch,†[ab] Mostafa Ronaghi†[b] and Juan G. Santiago*[a]

Received 19th February 2009, Accepted 14th April 2009
First published as an Advance Article on the web 28th April 2009
DOI: 10.1039/b903542g

We present a technique which enables the separation of small RNAs—such as microRNAs (miRNAs), short interfering RNAs (siRNAs), and Piwi-interacting RNAs (piRNAs)—from ≥66 nucleotide RNAs and other biomolecules contained in a cell lysate. In particular, the method achieves separation of small RNAs from precursor miRNAs (pre-miRNAs) in less than 3 min. We use on-chip isotachophoresis (ITP) for the simultaneous extraction, isolation, preconcentration and quantitation of small RNAs (~22 nucleotides) and employ the high-efficiency sieving matrix Pluronic F-127; a thermo-responsive triblock copolymer which allows convenient microchannel loading at low temperature. We present the isolation of small RNAs from the lysate of 293A human kidney cells, and quantitate the number of short RNA molecules per cell to be 2.9×10^7. We estimate this quantity is an aggregate of roughly 500 types of short RNA molecules per 293A cell. Currently, the minimal cell number for small RNA extraction and detection with our method is ~900 (from a 5 μL sample volume), and we believe that small RNA analysis from tens of cells is realizable. Techniques for rapid and sensitive extraction and isolation of small RNAs from cell lysate are much-needed to further uncover their full range and functionality, including RNA interference studies.

Introduction

There are three classes of small regulatory RNAs—siRNAs, miRNAs and piRNAs—and they are distinct in their biogenesis and cellular roles.[1] siRNAs are generated from double-stranded RNAs (dsRNAs) which are cleaved to ~21–25 nucleotides (nt) by Dicer, an endonuclease belonging to the RNaseIII family serving as a molecular ruler.[2] By contrast, miRNAs are derived in a two-step process. The primary precursors of miRNAs (pri-miRNAs) are encoded in the genome, having lengths of several hundred to thousands of nucleotides. In animals, the pri-miRNAs are then processed to ~70 nt pre-miRNAs which are transported into the cytoplasm, where the pre-miRNAs are cleaved to produce mature ~21–25 nt miRNA-miRNA* duplexes (where miRNA is the antisense, or guide, strand, and miRNA* is the sense, or passenger, strand).[3] Biogenesis of the third class, piRNAs which are single-stranded RNAs (ssRNAs) and ~24–31 nt long, is distinct from that of siRNAs and miRNAs and does not involve dsRNA precursors.[1]

RNA interference (RNAi) refers to the regulation of gene expression, in which small RNAs mediate gene silencing. In the RNAi process small RNAs are loaded onto Argonaute proteins at the core of an RNA-induced silencing complex (RISC), where these noncoding RNAs guide the sequence-specific silencing of transcripts through base-pairing interactions. The transcripts are typically messenger RNAs (mRNAs), which are cleaved or prevented from being translated by ribosomes, leading to their degradation. In humans at least 30% of the genes are thought to be regulated by miRNAs,[4] which tune protein synthesis from thousands of genes.[5,6] Further, miRNAs have recently been linked with common diseases.[7]

The gold standard of miRNA expression profiling is northern blotting,[8] although this technique involves laborious, time consuming procedures and lacks automation. The method of reverse transcription polymerase chain reaction (RT-PCR) is typically restricted to the quantitation of specifically lengthened miRNAs or pre-miRNAs, because the short length of miRNAs significantly limits the flexibility of primer design.[9,10] Microarrays allow profiling miRNAs in a highly efficient parallel fashion,[9,10] but this technique has encountered difficulties in reliably amplifying miRNAs without bias.

To overcome the obstacle of selective and sensitive quantitation devices for miRNA research, various techniques have been developed: a nanogapped microelectrode-based biosensor array;[11] electrocatalytic nanoparticle tags[12] and gold nanoparticle probes;[13] and capillary electrophoresis with the sieving matrices of poly(ethylene oxide)[14] or poly(vinyl pyrrolidone)[15] for miRNAs, and poly (ethylene glycol)[16] for general oligonucleotides applications.

Compared to conventional capillary electrophoresis, microchip electrophoresis techniques offer considerably shorter analysis times, the ability to work with small sample volumes, and the opportunity of combination with additional on-chip assay steps. However, the loading of microchannels with gels remains challenging due to the high viscosity of crosslinked gels and consequential bubble formation. Further, the separation of small nucleic acids in short microchannels requires a highly-efficient sieving medium. These challenges are at least partially

[a]*Department of Mechanical Engineering, Stanford University, Stanford, CA, 94305, USA. E-mail: juan.santiago@stanford.edu; Fax: +1 (650) 723 7657; Tel: +1 (650) 723 5689*
[b]*Stanford Genome Technology Center, Stanford University, Palo Alto, CA, 94304, USA*
† Current address: Illumina Inc., Corporate Headquarters, 9865 Towne Centre Drive, San Diego, CA 92121, USA.

addressed with the matrix Pluronic F-127, a thermo-responsive triblock copolymer which has a low viscosity at low temperature, allowing rapid microchannel loading. At room temperature and above, the uncrosslinked Pluronic F-127 forms a liquid crystalline phase, favorable for the separation of oligonucleotides[17] and DNAs[18,19] in microchips with channel lengths of a few cm.

ITP has been widely used as an electrophoretic separation technique[20] and is also a robust preconcentration method.[21,22] ITP employs a leading electrolyte (LE) and a trailing electrolyte (TE) whose mobilities are typically higher and lower, respectively, than the mobilities of sample species. This technique enables analysis of a variety of compounds, ranging from small molecules such as metal ions to large biomolecules like proteins. The combination of ITP with subsequent separation by gel electrophoresis allows high-sensitivity detection of DNA fragments.[23–25]

In this paper, we demonstrate the extraction, isolation, preconcentration, and quantitation of small RNAs from cell lysate using ITP in microchannels loaded with the high-efficiency sieving medium Pluronic F-127. First, we show the efficiency of this sieving matrix in our chip by separating short DNA ladders *via* transient ITP. Then, we perform fundamental ITP demonstration experiments with 22 and 66 nt oligos, which have very similar physical properties to small RNAs and pre-miRNAs, respectively, and are less susceptible to RNase degradation. Finally, we present that our technique separates actual small RNAs from pre-miRNAs, large mRNAs, ribosomal RNAs (rRNAs), and other biomolecules contained in the lysate of 293A cells from the human kidney. From these results we estimate the number of different types of small RNAs per cell. Currently, commercial kits only allow the separation of small RNAs from >200 nt RNAs, and we present the separation of small RNAs from pre-miRNAs and other RNA molecules ≥66 nt. Our technique should therefore aid in increasing the expression analysis sensitivity of small RNAs, and facilitate the identification of the full range of small RNAs, assisting RNAi studies.

Experimental

Chemicals and reagents

6-Aminocaproic acid, caproic acid, Tris, Bis-Tris, HEPES, Pluronic F-127 (registered trademark of BASF), Igepal CA-630, and sodium chloride were purchased from Sigma-Aldrich (St. Louis, MO). HCl and magnesium chloride hexahydrate were from EMD Chemicals (Gibbstown, NJ). 22 nt and 66 nt oligos (both mixed base A, C, G) were from Integrated DNA Technologies (Coralville, IA). SYBR Green I and II; 50 base pairs (bp), 123 bp, and 250 bp DNA ladders; 0.1–2 kb RNA ladder; 293A cell line; streptavidin (Alexa Fluor 488 conjugate); albumin from bovine serum (BSA, Alexa Fluor 488 conjugate); and ultrapure DNase/RNase-free distilled water were purchased from Invitrogen (Carlsbad, CA). The 10 bp DNA ladder was from Promega (Madison, WI). We purchased embryonic kidney (293) total RNA, RNase inhibitor, and RNaseZap wipes from Ambion (Austin, TX).

Cell lysate preparation

Cell lysing was preformed off-chip according to the following typical procedure. We followed the first three steps of the RNeasy Mini Kit supplementary protocol from QIAGEN (Hilden, Germany). First, 3×10^6 293A cells were pelleted by centrifuging for 5 min at 300g and the supernatant was removed by aspiration. Second, the cells were resuspended in 175 μL of precooled (4 °C) lysis buffer and incubated for 5 min on ice. The lysis buffer contained 50 mM Tris and 30 mM HCl (pH 8), 140 mM NaCl, 1.5 mM $MgCl_2$, 0.5% (v/v) Igepal CA-630 which is a nonionic detergent, and just before use we added 1 U μl^{-1} RNase inhibitor. Third, we centrifuged the cell lysate at 4 °C for 2 min at 300g and recovered the supernatant which contained the cell lysate.

Electrolyte composition

We experimented with and evaluated the performance of 55 ITP buffer combinations[26] and several labeling techniques. Here, we describe our experiments with the best performing chemistry. We used chloride ions as an LE. The LE buffer was 140 mM 6-aminocaproic acid and 100 mM HCl (pH 4). The TE was 10 mM 6-aminocaproic acid and 50 mM caproic acid (pH 4), and this anion mobility allows the separation of small RNAs from pre-miRNAs. At pH 4 of the LE and TE, 6-aminocaproic acid is the counterion. We chose this counterion because one of its pK_a values is ~4.4, allowing for the design of the LE and TE to be near pH 4. This value was attractive because at pH 4 most proteins contained in the cell lysate are positively charged since they have a pI > 4.[27] Thus, most proteins do not migrate through the microchannel and remain in the sample reservoir. We verified the latter with a set of preliminary experiments using streptavidin and albumin from bovine serum (each labeled with Alexa Fluor 488).

The pH values of the electrolytes were measured with Corning Pinnacle 542 pH/conductivity meter from Nova Analytics (Woburn, MA). All buffers were prepared with distilled, ultrapure, 0.1 micron filtered, RNase and DNase free water, and contained the intercalating dye SYBR Green I (for dsDNA) or SYBR Green II (for RNA) at 1× concentrations. For the experiments with lysed 293A cells we worked at concentrations of 100× SYBR Green I and II. These intercalating dyes are positively charged when they are free in solution, and so conveniently do not focus in our anionic ITP experiments. SYBR Green I and II have a much lower fluorescence quantum yield when free in solution than when complexed with either dsDNA or RNA.[28] These dyes are used effectively in a variety of analytical and diagnostic applications for the detection of nucleic acids.[29]

Sieving matrix

For the separation of 22 nt from 66 nt oligos we have chosen Pluronic F-127 at a concentration of 30% (w/v), which has demonstrated to be highly effective for the sieving of oligos with lengths of 8–32 nt.[17,30] The triblock copolymer was dissolved in the LE and placed in the refrigerator (4 °C) for a few days prior use to ensure complete dissolution of the powder.

Imaging

For imaging we used the inverted epifluorescent microscope IX70 from Olympus (Hauppauge, NY), equipped with a 100 W mercury lamp, a 10× UPlanFl objective (NA 0.3), a 0.63× non-parfocalizing adapter, and a XF115-2 filtercube (455–490 nm excitation, 510 nm emission, 505 nm cutoff dichroic) from Omega Optical (Brattleboro, VT). Images were captured with a MicroMax 1300 CCD camera controlled with WinView32, both from Princeton Instruments (Trenton, NJ). For image analysis we used ImageJ from the National Institute of Health and MATLAB from MathWorks (Natick, MA).

On-chip isotachophoresis experiments

We performed all experiments on NS-95 glass microchips from Caliper (Mountain View, CA), having a simple-cross geometry with wet-etched 12 μm deep by 34 μm wide channels. Fig. 1 shows a schematic of chip and experimental steps. The separation channel from the west well to the cross has a length of 27.5 mm. For loading the separation channel with Pluronic F-127 the chip was placed in the freezer (−10 °C) for 10 min. We then loaded the north and south reservoirs with LE buffer and the west well with refrigerated Pluronic F-127 solution (T ≈ 4 °C), and applied a vacuum at the east reservoir for 2 min (Fig. 1(a)). Since the resistance of the north and south channels is much lower than that of the west channel, the Pluronic F-127 sieving matrix effectively only fills the west channel. The east channel is filled primarily with LE. (Some small amount of Pluronic F-127 is drawn into the east as thin stream, but this Pluronic F-127 "fiber" was negligibly small and often not detectable.) After vacuum-assisted channel loading the remaining sieving solution was removed from the west well by aspiration with a pipette tip and vacuum line, and refilled with LE to guarantee repeatable results. We let the system warm up to room temperature for 10 min, during which period Pluronic F-127 formed a crystalline phase.

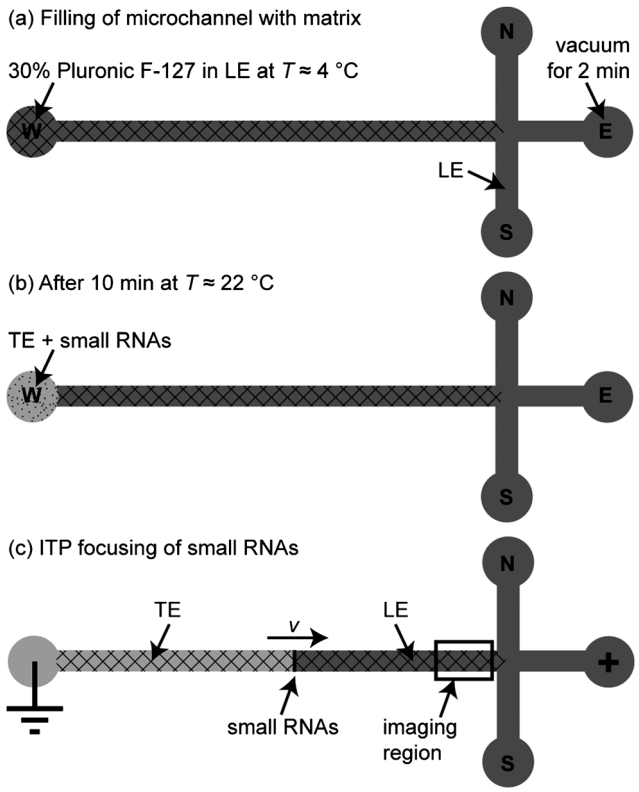

Fig. 1 Schematics of the microchip and description of protocol for loading Pluronic F-127, and extracting, isolating, preconcentrating, and quantitating small RNAs using ITP. The microchip is first placed in the freezer for 10 min. Then, the north and south reservoirs are filled with LE, and the west well with refrigerated 30% Pluronic F-127. (a) For filling the microchannels with solutions, a vacuum is applied at the east reservoir for 2 min, and immediately thereafter the west well is cleaned and refilled with LE. (b) After a 10 min warm-up period, Pluronic F-127 transitions into a high-viscosity solution, and the west reservoir is filled with TE and small RNAs. (c) The separation and focusing of small RNAs is initiated by applying the anode in the east well and the cathode in the west reservoir. The ITP zone travels with the velocity $v(t)$ downstream. Small RNAs are detected just to the left of the intersection as indicated.

After the warm-up period, we performed a pre-run at an electric field strength of 200 V cm^{-1} to stabilize the sieving matrix. For the application of the electric field we used the LabVIEW-controlled high-voltage power supply Microfluidic Tool Kit from Micralyne (Edmonton, AB, Canada) and placed platinum wires in the east and west reservoirs. Then, the LE in the west well was replaced by a mixture of TE and sample (Fig. 1(b)), and the electric field of 400 V cm^{-1} was applied in the east–west direction. As shown in Fig. 1(c), the sample zone is focused between the LE and TE and travels with the velocity $v(t)$ downstream,[31] increasing in concentration and amount of sample with time as the ITP is in peak mode.[32] (Note the ITP velocity is approximately constant within the 1.2 mm wide detection region even at potentiostatic conditions.) Fluorescence signals were collected at the end of the separation channel just to the left of the cross. After each experiment Pluronic F-127 was removed from the separation channel by refrigerating the device and applying a vacuum at the west reservoir for a few minutes. Then, we cleaned the device with 0.1 M KOH for 15 min and thereafter with distilled, ultrapure water. Additionally, when working with 293 total RNA or 293A cell lysate, we cleaned all surfaces with RNaseZap wipes to ensure an RNase-free environment.

Transient isotachophoresis

The sieving efficiency of Pluronic F-127 was investigated and demonstrated using transient ITP (tITP). tITP first preconcentrates samples in a preliminary ITP step. The ITP step is then interrupted by injecting LE ions behind the TE region, and this initiates electrophoretic separation of analytes. We used a tITP protocol similar to that described by Bharadwaj *et al.*[33] To load the sieving matrix we followed the same procedure as described in Fig. 1, but for tITP experiments the TE was 10 mM Bis-Tris and 50 mM HEPES (pH 6.5). This TE has a lower mobility than that for the other ITP experiments, hence also focusing relatively low mobility species such as long nucleic acids, for example. After a few seconds of ITP preconcentration we turned off the electric field, quickly replaced the solution in the west reservoir with LE, and applied an electric field of 1200 V cm^{-1}. This way, the ITP mode is terminated by injecting LE into the separation channel. Leading ions overtake first trailing ions and then sample

ions, thus initiating a separation of sample species by capillary electrophoresis.

Results and discussion

On-chip sieving matrix performance

There exists a difference in the mobility between 22 nt and 66 nt DNAs in free solution,[34] but this difference is small and we found it difficult to exploit for selective isolation of small RNAs. We therefore employed the molecular sieving matrix Pluronic F-127 to enhance the sensitivity of nucleic acid length on mobility. Pluronic F-127 is a triblock copolymer PEO-PPO-PEO, where PPO is poly(propylene oxide) and PEO is poly(ethylene oxide). At temperatures below 15 °C the viscosity of this amphiphilic copolymer solution is low because PPO is hydrophilic,[19] and Pluronic F-127 dissolved in water acts as a free flowing solution.[30] When the temperature is increased, the hydrogen bonds between PPO and water are broken, leading to a high degree of PPO hydrophobicity so that micelles are formed. These spherical micelles with hydrophobic PPO cores surrounded by PEO brushes are packed in a face-centered cubic nanostructure, forming a liquid crystalline phase.[35] It was measured for 20% Pluronic F-127 that the viscosity at 4 °C is ~50 cP compared to a value of ~900 cP at 22 °C.[19]

This high-efficiency sieving matrix has been used effectively for the separation of nucleic acids over a wide range of sizes: oligos of 5–60 nt,[30,35] DNA fragments of 25–1500 bp,[18,19] and supercoiled plasmid DNAs of 2–10 kbp.[35,36] Since Pluronic F-127 effectively suppresses electro-osmotic flow,[37] electrophoresis is the dominant transportation mode. Unfortunately, a general, physical sieving mechanism has not yet been described in this matrix.[38]

To demonstrate the efficacy of 30% Pluronic F-127, we analyzed the separation of nucleic acids using tITP. Fig. 2(a) shows the separation of a 10–100 bp DNA ladder (with 10 bp increments). 8 of the 10 fragments were detected without optimization of tITP conditions. According to the supplier, the 10 bp band appears slightly less intense than the other bands (hence the high mobility peak 1 in Fig. 2(a)). Further, we separated a 50–800 bp DNA ladder (with 50 bp increments, and a vector fragment >2 kbp) as demonstrated in Fig. 2(b), and here resolved 15 out of 17 fragments. The 350 bp band is designed by the supplier to be two- to three-times brighter than neighboring bands (hence we identify the intermediate-mobility peak 7 in Fig. 2(b)). Peak 15 is likely the low-mobility 2652 bp DNA fragment.

Although the DNA ladders shown in Fig. 2 are not perfectly resolved, these experiments confirm that the sieving matrix imparts a significant dependence of electrophoretic mobility on nucleotide length. Below, we demonstrate how we leverage this dependence in selective isolations of small RNAs *via* ITP focusing.

Isotachophoresis extraction and isolation

In typical ITP, analytes at sufficiently high concentration (and after sufficient focusing time) segregate into distinct zones characterized by a plateau at steady state.[20] The composition of plateau zones is described fairly generally by the Alberty[39] and Jovin[40] functions governing ITP electromigration dynamics.

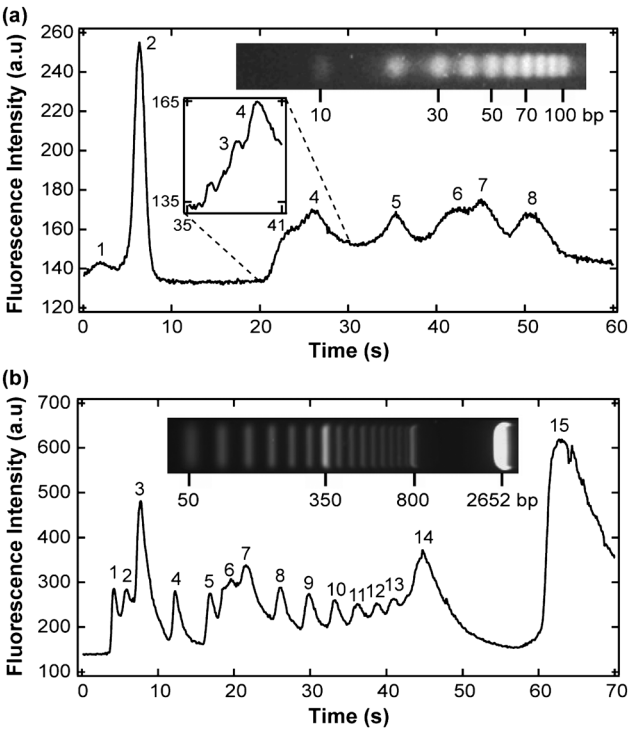

Fig. 2 Separation of short DNA ladders in 30% Pluronic F-127 using tITP. (a) 8 out of 10 fragments were resolved from a 10–100 bp DNA ladder. The inset shows the magnification of peak 3 and 4, measured further downstream. (b) For the 50–800 bp DNA ladder 15 out of 17 fragments were detected. The LE was 140 mM 6-aminocaproic acid with 100 mM HCl, and the TE was 10 mM Bis-Tris and 50 mM HEPES. The dye was 1× SYBR Green I, and the electric field strength for separation was 1200 V cm^{-1}. The images (from the suppliers) in (a) and (b) show the separation of the DNA ladders in 4% and 2% agarose gels, respectively.

However, analytes at initially trace concentrations rarely have sufficient time (or channel length) to achieve plateau zones. Such analytes focus into approximately Gaussian peaks, and this regime is thus called peak mode ITP.[32] Khurana and Santiago[41] presented a theoretical and experimental study for the electrolyte composition optimization in the peak mode regime. We followed their guidelines in designing our ITP system chemistry, which is summarized in Table 1.

The selection of the electrolyte system is crucial since this allows us to selectively extract and isolate small RNAs from a large variety of other biomolecules present in the cell lysate, including but not limited to pre-miRNAs, mRNAs, rRNAs, DNAs, and proteins. The mobility of small RNAs in our sieving matrix decreases with increasing number of nucleotides. We have searched for and found an effective mobility for our TE which is between the mobility of small RNAs and pre-miRNAs in the sieving matrix, hence separating these species. Again, Table 1 shows the system parameters of the LE and TE; these were determined from simulations using Peakmaster 5.2 for the buffer calculations (including ionic strength dependence).[42] The current density was typically ~2.45×10^4 A m^{-2}, and this gave sufficient buffering capacity. The minimal ionic strength was ~8 mM during a 5 min ITP experiment and the reservoir size was 5 μL. Therefore, we estimate a change of pH of less than ~0.2 using the Henderson–Hasselbach equation.[43,44]

Table 1 System parameters of the leading and trailing electrolyte ions.[42] Shown are total concentration; abbreviated name; fully-ionized mobility magnitude and associated valence; pK_a value and corresponding valences; and effective mobility (calculated using Peakmaster[42]) of the relevant ions. The sign of the effective mobility indicates the sign of the valence at the relevant local pH

	Conc. (mM)	Abbr.	(Valence) Mobility ($m^2\ V^{-1}\ s^{-1}$)	pK_a (Valences)	Eff. mobility ($m^2\ V^{-1}\ s^{-1}$)
LE	140	6ACA[a]	(+1) 29×10^{-9}	4.4 (+1,0)	15×10^{-9}
	100	HCl	(−1) 79×10^{-9}	−2 (0,−1)	-68×10^{-9}
TE	10	6ACA[a]	(+1) 29×10^{-9}	4.4 (+1,0)	18×10^{-9}
	50	CA[b]	(−1) 30×10^{-9}	4.9 (0,−1)	-4×10^{-9}

[a] 6-Aminocaproic acid. [b] Caproic acid.

Fig. 3 shows a demonstration experiment where we separated 22 nt from 66 nt oligos, which consisted of only A, C, and G bases. These species have physical properties very similar to small RNAs and pre-miRNAs, respectively. Only 22 nt oligos are focused by ITP as shown by our spiking procedure and control experiments. In all of the experiments shown, the mobility of the TE is higher than our estimates of mobility for oligos of equal or longer length than 66 nt. The top trace shows the baseline control case where no oligos are present. Adding 100 nM of 66 nt oligos results in only a small peak (near 145 s), which we attribute to shorter-oligo impurities from the 66 nt oligo sample (the supplier reports that the sample contains 7% shorter fragments remaining after their purification of the nominal 66 nt oligo sample from polyacrylamide gel electrophoresis). Next, the sample with 10 nM 22 nt oligos and 100 nM 66 nt oligos shows a dramatically increased peak height near 142 s. Spiking the 22 nt oligo sample (100 nM 22 nt oligos and 100 nM 66 nt oligos) clearly results in the increase of the peak (now at 138 s) which we therefore identify as 22 nt oligos. This spiking shows that the fluorescence intensity of the peak identified as 22 nt oligos is proportional only to the starting concentration of that species, which is further confirmed in the bottom trace which is spiked with 100 nM 22 nt oligos only. For these experiments, labeled oligos >66 nt (which do not focus) undergo moving boundary electrophoresis[45] and so result in a slight upward drift in the background signal value starting at about 150 s (see the second through fourth traces of Fig. 3).

Next, we present the separation of 22 nt oligos from a 0.1–2 kb RNA ladder in Fig. 4. The fluorescence intensity is proportional to the starting concentration of 22 nt oligos, which focus in the ITP zone between the LE and TE. Note for example the third trace from the top which contained both 22 nt oligos and 0.1–2 kb RNA ladder. Spiking 22 nt oligos at concentrations of 10, 100 and then 1000 nM progressively increases the associated peak intensity (and integrated area) as expected. Again, we attribute the slight peak near 142 s in the top trace to impurities from the RNA ladder.

Having shown the separation of 22 nt oligos from 66 nt oligos and a 0.1–2 kb RNA ladder, we here demonstrate that our ITP-based technique can indeed extract, separate and preconcentrate small RNAs from pre-miRNAs and other biomolecules in lysate of 293A cells. Fig. 5 summarizes the results of the control, extraction, and spiking experiments. As before, we have shifted the traces in time (here by 5 s) for clarity. The experiments shown in Fig. 5 used 100× SYBR Green II, except for the second trace (from the top) which used 100× SYBR Green I. In the second and third electropherogram, we show that small RNAs from the

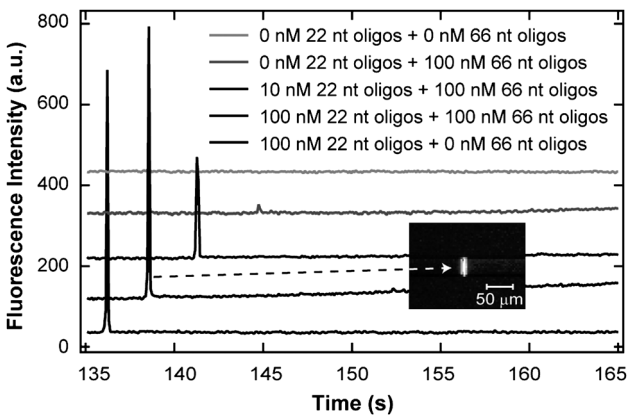

Fig. 3 ITP-based extraction and separation of 22 nt from 66 nt oligos in 30% Pluronic F-127. The measured signal is dependent only on the 22 nt oligo concentration and independent of the 66 nt oligos. The fluorescence image shows 100 nM 22 nt oligos which are highly focused by ITP in the microchannel. These experiments suggest that our technique is capable of separating small RNAs from pre-miRNAs as further demonstrated in Fig. 5. The traces are shifted in time by ~2.5 s (major peaks otherwise approximately line up) and fluorescence intensity to facilitate their comparison.

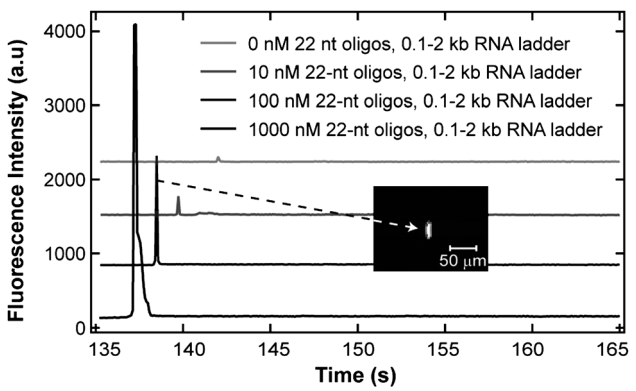

Fig. 4 Extraction and separation of 22 nt oligos from a 0.1–2 kb RNA ladder (all at 10 μg ml^{-1}) by ITP in 30% Pluronic F-127. We confirm that short oligo (near 22 nt) are selectively isolated from the RNA ladder by a series of spiking experiments. The sharp peak of 100 nM 22 nt oligos is shown in the fluorescence image. The traces are again shifted in time (here by ~2 s) and fluorescence intensity to aid in comparison.

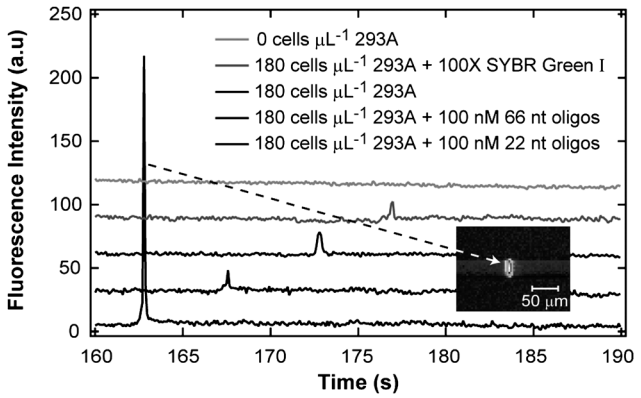

Fig. 5 Extraction, isolation and preconcentration of small RNAs from 293A cell lysate using on-chip ITP in a channel loaded with 30% Pluronic F-127. Only 22 nt oligos and not 66 nt oligos spiked in the cell lysate are focused by ITP, demonstrating that small RNAs are separated from pre-miRNAs. Focused small RNAs which are separated from pre-miRNAs and ≥66 nt RNAs are shown in the second, third, and fourth traces. The fluorescence image shows an ITP peak of spiked 22 nt oligos and small RNAs from the cell lysate. The dye was 100× SYBR Green II, except for the second trace from the top where we used only 100× SYBR Green I. The traces are shifted in time (by 5 s) and fluorescence intensity to allow their comparison.

lysate of 293A cells (at a concentration of 180 cells μL^{-1}) were detected with SYBR Green I and II, respectively. SYBR Green I (designed to bind to dsDNA) intercalates into RNA at a lower quantum yield than SYBR Green II.[29] Consistently, the RNA peak in the third trace has a 15% higher peak height. Spiking the cell lysate with 100 nM 66 nt oligos (fourth trace) results in the same peak shape and intensity for the presumed short (near 22 nt) RNA peak, as expected. Perhaps the strongest evidence is offered by the fifth trace which shows an 11.7 fold signal increase when we spike the lysate with (non-native) 100 nM 22 nt oligos. Note that the second, third, and fourth traces all have areas of the same order of magnitude, but spiking with 22 nt oligos definitely results in a dramatic increase in concentration. Clearly, the peak height of the isolated small RNA peak has a mobility below 66 nt and nearer to that of 22 nt RNAs. Although not shown here, we have also extracted, isolated and quantitated small RNAs from 10 μg ml^{-1} total RNA samples (processed from embryonic kidney cells (293)), and measured the associated peak heights at ∼255 a.u. We have also performed a series of additional calibration experiments with individual oligos and RNA ladders from which we conclude that our ITP extraction process has a cut off near 50 nt as the maximum RNA nucleotide length.

Next, we present an analysis by which we approximately quantify the amount of small RNAs in our 293A cell line. The bottommost trace of Fig. 5 was spiked with a known amount of 100 nM 22 nt oligos, and this peak is 11.7 higher intensity than the unspiked sample peak of the third trace, as per the expected, peak mode ITP physics.[41] We can therefore approximate the concentration of small RNAs in the original sample to be 8.6 nM.[46] Considering the concentration of 180 cells μL^{-1}, we obtain 2.9×10^7 small RNAs per cell. Earlier studies have suggested that the total number of piRNAs be on the order of a million fold, and miRNAs are expressed at high levels up to several ten thousands of copies per cell.[47] The total number of types of small RNAs per cell is not known,[1] but we can deduce it by taking the assumption that small RNAs are present at 6×10^4 copies per cell.[48] This results in an estimate of roughly 500 different types of small RNAs per 293A cell, out of which 122 are known today.[49]

We also considered the possibility that the ITP zone may contain other nucleic acids from the cell lysate which have a mobility nearly equal to that of small RNAs. We explored this issue by performing ITP experiments with the following three DNA ladders: 50–800 bp with vector fragment >2 kbp, 123–4182 bp, and 250–3500 bp. The ladders were labeled with SYBR Green I. These DNA experiments confirm that there is some focusing of fluorescent analyte in our ITP electrolyte system for all three ladders. The measured peak heights of the ITP zone for 50–800 bp, 123–4182 bp, and 250–3500 bp DNA ladders (all at 10 μg ml^{-1}) were ∼1290 a.u., ∼3960 a.u., and ∼1150 a.u., respectively. This suggests that our ITP method may be extracting and preconcentrating some DNA molecules which are not necessarily short (tens of bp) but long (several kbp). This result is consistent with previous separation studies using Pluronic F-127 which confirm that large plasmid dsDNA (2–10 kbp) may indeed (and perhaps counterintuitively) have mobilities near those of small RNAs.[36] Wan and coworkers hypothesized that this is due to the more rigid structure of DNA which can break down PEO bridges in Pluronic F-127 and lead to a temporary change in the lattice structure.[38] In contrast, single stranded nucleic acids are more flexible and believed to migrate through PEO meshes and interstitial domains without disrupting them. Thus, we concede the possibility that plasmid DNAs may also be focusing in our ITP experiments. However, we expect the majority of the preconcentrated nucleic acids in the peaks shown in Fig. 5 to be small RNAs, because the number of plasmid DNAs per cell is expected to be much fewer than the number of small RNAs. For example, Meyer *et al.*[50] reported a few tens of plasmid DNAs per cell. In any case, we recommend that implementations of our assay should include the treatment with DNase to degrade all DNA molecules, and hope to further explore this issue in the future.

Last, we note observations regarding ITP velocity which may aid in efforts to simulate the current assay and further analyze the physicochemical process. The ITP zone velocity was approximately constant during the time the ITP zone was in the imaging region. For the lysate containing samples, this velocity was reduced by a factor of ∼1.2 compared to samples containing only oligonucleotides. This is consistent with the increased detection time from ∼140 s (Fig. 3 and 4) to ∼170 s (Fig. 5), a ∼20% mobility reduction. This effect is most likely due to the high ionic strength of the cell lysate. We use the nonionic detergent Igepal CA-630 to reduce ionic strength, but the lysis buffer also contained 140 mM NaCl. Since we diluted the cell lysate 100 fold with the TE buffer (final ionic strength was 7 mM), the final NaCl concentration in the lysate sample was 1.4 mM (∼20%). Chloride is a strong electrolyte and faster than the TE, thus carrying at least 20% of the current and this acts to reduce the ITP velocity. The means and 95% confidence for peak arrival time at the end of the (27.5 mm) separation channel were 140 s ± 10% for samples without cell lysate, and 170 s ± 10% for samples in cell lysate.

Conclusions and recommendations

We introduced a rapid and sensitive ITP-based technique for the extraction, isolation, preconcentration, and quantitation of small RNAs from cell lysate. In this paper we demonstrated that the technique isolates RNAs with lengths of roughly 22 nt (in the range of miRNAs and siRNAs), and that its selective isolation rejects 66 nt and larger RNAs. We are able to quantitate small RNAs of only ~900 cells in ~5 μL, and we believe that the sensitivity can be decreased considerably, allowing small RNA extractions from tens of cells.

We can define the extraction efficiency as the ratio of the measured number of focused small RNAs in the ITP zone divided by the estimated number of small RNAs in the 5 μL sample reservoir. In turn, the amount of focused small RNAs in the ITP zone can be deduced from the preconcentration factor of our system (the latter is the final analyte concentration in the ITP peak divided by the initial sample concentration). We estimated preconcentration factors after 170 s using three methods. Analytically,[41] we estimate a preconcentration of 5.3×10^4 fold. Using the open-source simulation tool Spresso described by Bercovici *et al.*,[51] we estimate 6.8×10^4 fold.[52] Experimentally, we measure a value of 4.1×10^4 fold. The latter is determined by analyzing the detected intensities of the ITP zone in controlled spiking experiments where the initial oligo concentration is well known. Assuming a nominal expected preconcentration factor ranging from 4×10^4 to 5×10^4 fold, we estimate an extraction efficiency of 5 to 6%. In our current device design, this value is limited by channel geometry and electromigration rate. We expect that this efficiency can be improved to near 100% by increasing the cross-sectional area of the microchannel in both dimensions. For example, an increase in both channel width and depth of a factor of 10 should achieve near complete extraction (neglecting losses due to adsorption, *etc.*). The current density of the current experiments is order 2.5×10^4 A m^{-2}, so we estimate that Joule heating will not be a limiting factor.

Our technique of on-chip ITP-based extraction, isolation, preconcentration, and quantitation of small RNAs likely has relevance for various biotechnological applications. We believe it is a promising method for isolation of various nucleic acids, and the chemistry and methods should be compatible with a variety of devices. In future work, we hope to be able to couple this technique with additional assay and evaluation steps on a chip. In particular, our method may facilitate small RNA silencing studies which aim to study differential expression and regulatory roles of small RNA on common diseases.

Acknowledgements

We gratefully acknowledge funding from the Stanford Genome Technology Center, the National Institute of Health under Grant N01-HV-28183, and the U.S. Department of Energy by Lawrence Livermore National Laboratory under Contract DE-AC52-07NA27344. The authors thank Robert D. Chambers, Moran Bercovici, Tarun Khurana, and Alexandre Persat from the Microfluidics Laboratory; AmirAli H. Talasaz from the Genome Technology Center, and Zhihai Ma from the Department of Pathology for fruitful discussions and constructive comments.

References

1 H. Siomi and M. C. Siomi, *Nature*, 2009, **457**, 396–404.
2 M. Jinek and J. A. Doudna, *Nature*, 2009, **457**, 405–412.
3 N. Bushati and S. M. Cohen, *Annu. Rev. Cell Dev. Bi.*, 2007, **23**, 175–205.
4 B. P. Lewis, C. B. Burge and D. P. Bartel, *Cell*, 2005, **120**, 15–20.
5 M. Selbach, B. Schwanhausser, N. Thierfelder, Z. Fang, R. Khanin and N. Rajewsky, *Nature*, 2008, **455**, 58–63.
6 D. Baek, J. Villen, C. Shin, F. D. Camargo, S. P. Gygi and D. P. Bartel, *Nature*, 2008, **455**, 64–71.
7 J. Couzin, *Science*, 2008, **319**, 1782–1784.
8 V. Ambros *et al.*, *RNA*, 2003, **9**, 277–279.
9 P. T. Nelson, D. A. Baldwin, L. M. Scearce, J. C. Oberholtzer, J. W. Tobias and Z. Mourelatos, *Nat. Methods*, 2004, **1**, 155–161.
10 C.-G. Liu *et al.*, *Proc. Natl. Acad. Sci. USA*, 2004, **101**, 9740–9744.
11 Y. Fan, X. T. Chen, A. D. Trigg, C. H. Tung, J. M. Kong and Z. Q. Gao, *J. Am. Chem. Soc.*, 2007, **129**, 5437–5443.
12 Z. Gao and Z. Yang, *Anal. Chem.*, 2006, **78**, 1470–1477.
13 W. J. Yang *et al.*, *Anal. Biochem.*, 2008, **376**, 183–188.
14 P.-L. Chang, Y.-S. Chang, J.-H. Chen, S.-J. Chen and H.-C. Chen, *Anal. Chem.*, 2008, **80**, 8554–8560.
15 N. Li, A. Nguyen, J. Diedrich and W. Zhong, *J. Chromatogr. A*, 2008, **1202**, 220–223.
16 R. Chen, X. F. Luo, X. Di, Y. Li, Y. Q. Sun and Y. Z. Hu, *J. Chromatogr. B*, 2006, **843**, 334–338.
17 J. Zhang, M. Gassmann, W. D. He, F. Wan and B. Chu, *Lab Chip*, 2006, **6**, 526–533.
18 V. M. Ugaz, R. S. Lin, N. Srivastava, D. T. Burke and M. A. Burns, *Electrophoresis*, 2003, **24**, 151–157.
19 D. Kuroda, Y. Zhang, J. Wang, N. Kaji, M. Tokeshi and Y. Baba, *Anal. Bioanal. Chem.*, 2008, **391**, 2543–2549.
20 A. J. P. Martin and F. M. Everaert, *Anal. Chim. Acta*, 1967, **38**, 233–237.
21 S. L. Simpson, J. P. Quirino and S. Terabe, *J. Chromatogr. A*, 2008, **1184**, 504–541.
22 B. Jung, R. Bharadwaj and J. G. Santiago, *Anal. Chem.*, 2006, **78**, 2319–2327.
23 A. Wainright, U. T. Nguyen, T. Bjornson and T. D. Boone, *Electrophoresis*, 2003, **24**, 3784–3792.
24 Z. Q. Xu, T. Hirokawa, T. Nishine and A. Arai, *J. Chromatogr. A*, 2003, **990**, 53–61.
25 C. C. Lin, B. K. Hsu and S. H. Chen, *Electrophoresis*, 2008, **29**, 1228–1236.
26 We performed different LE-TE combinations in both free solution(35 combinations) and in the Pluronic F-127 sieving matrix (20 combinations). We used 9 combinations of electrolyte pH values using 50 weak electrolyte buffers and slight variations in titration of some of these buffers. In 10 cases we varied ionic strength.
27 H. M. Georgiou, G. E. Rice and M. S. Baker, *Proteomics*, 2001, **1**, 1503–1506.
28 G. Cosa, K. S. Focsaneanu, J. R. N. McLean, J. P. McNamee and J. C. Scaiano, *Photochem. Photobiol.*, 2001, **73**, 585–599.
29 H. Zipper, H. Brunner, J. Bernhagen and F. Vitzthum, *Nucleic Acids Res.*, 2004, **32**, e103.
30 J. Zhang, D. H. Liang, W. D. He, F. Wan, O. C. Ying and B. Chu, *Electrophoresis*, 2005, **26**, 4449–4455.
31 S. V. Ermakov, M. Y. Zhukov, L. Capelli and P. G. Righetti, *Electrophoresis*, 1995, **16**, 2149–2158.
32 S. J. Chen, S. W. Graves and M. L. Lee, *J. Microcolumn Separations*, 1999, **11**, 341–345.
33 R. Bharadwaj, D. E. Huber, T. Khurana and J. G. Santiago, in *Handbook of Capillary and Microchip Electrophoresis and Associated Microtechniques*, ed. J. P. Landers, CRC Press, 3rd edn., 2008, ch. 38, pp. 1085–1120.
34 E. Stellwagen, Y. J. Lu and N. C. Stellwagen, *Biochemistry*, 2003, **42**, 11745–11750.
35 R. L. Rill, Y. J. Liu, D. H. Van Winkle and B. R. Locke, *J. Chromatogr. A*, 1998, **817**, 287–295.
36 R. L. Rill, Y. Liu, B. A. Ramey, D. H. Van Winkle and B. R. Locke, *Chromatographia*, 1999, **49**, S65–S71.
37 C. Wu, T. Liu and B. Chu, *Electrophoresis*, 1998, **19**, 231–241.
38 F. Wan, J. Zhang, A. Lau, S. Tan, C. Burger and B. Chu, *Electrophoresis*, 2008, **29**, 4704–4713.
39 R. A. Alberty, *J. Am. Chem. Soc.*, 1950, **72**, 2361–2367.

40 T. M. Jovin, *Biochemistry*, 1973, **12**, 871–878.
41 T. K. Khurana and J. G. Santiago, *Anal. Chem.*, 2008, **80**, 6300–6307.
42 M. Jaros, V. Hruska, M. Stedry, I. Zuskova and B. Gas, *Electrophoresis*, 2004, **25**, 3080–3085.
43 L. J. Henderson, *Am. J. Physiol.*, 1908, **21**, 173–179.
44 A. Persat, T. A. Zangle, J. D. Posner and J. G. Santiago, *Lab Chip, Chips & Tips*, 26 March, 2007.
45 J. L. Beckers and P. Bocek, *Electrophoresis*, 2000, **21**, 2747–2767.
46 In Figs. 3 and 4, the peak intensity is not a linear function of initial sample concentration as the focused concentration is ~5 mM or larger where fluorescence quenching is likely.[29] However, for initial oligo concentrations of 100 nM or less in lysate (lower fluorescence signals than in pure oligonucleotide samples) we expect the fluorescence signal to be linear with the sample concentration, and therefore use this assumption for the approximation of the small RNA concentration in the ITP zone.
47 T. A. Farazi, S. A. Juranek and T. Tuschl, *Development*, 2008, **135**, 1201–1214.
48 D. Haussecker, D. Cao, Y. Huang, P. Parameswaran, A. Z. Fire and M. A. Kay, *Nat. Struct. Mol. Biol.*, 2008, **15**, 714–721.
49 P. Landgraf *et al.*, *Cell*, 2007, **129**, 1401–1414.
50 R. Meyer, M. Hinds and M. Brasch, *J. Bacteriol.*, 1982, **150**, 552–562.
51 M. Bercovici, S. K. Lele and J. G. Santiago, *J. Chromatogr. A*, 2009, **1216**, 1008–1018.
52 These calculations and simulations were performed given free solution values for the (small) buffer ions, but in our experience this assumption yields focusing ratios approximately equal to those measured in Pluronic F-127.

